Dynamic graph analysis reveals aging effects on motor network communication

Nils Rosjat[1,2*], Bin A. Wang[1], Liqing Liu[1,2], Gereon R. Fink[1,3], Silvia Daun[1,2]

1 Cognitive Neuroscience, Institute of Neuroscience and Medicine (INM-3), Forschungszentrum Jülich, Jülich, Germany

2 Institute of Zoology, University of Cologne, Cologne, Germany

3 Department of Neurology, Faculty of Medicine and University Hospital Cologne, University of Cologne, Cologne, Germany

* n.rosjat@fz-juelich.de

Abstract

The vast majority of our actions, including their preparation and execution, result from a complex interplay of brain regions. To date our knowledge of aging-associated functional changes in the motor networks, which are known to impact motor performance, remains sketchy. In this study, we generated and analyzed dynamical graphs based on phase-locking of EEG signals recorded from healthy right-handed younger (YS) and older subjects (OS) while they performed a simple finger-tapping task. The network analysis yielded four major results: An underlying coupling structure around movement onset in the low frequencies (2-7 Hz) present in YS and OS. The network in OS, however, contained several additional

connections, in particular interhemispheric ones, and showed an overall increased coupling density, which was supported by significantly increased node degrees. Louvain clustering, the calculation of the variance of information, and the node flexibility revealed reduced variability of the subnetworks in OS, particularly during movement preparation. The analysis of hub nodes showed a strong involvement of occipital, parietal, sensorimotor, and central regions in YS. In OS, the first occurrence of sensorimotor hubs was noticeably delayed and preceded by a hub in frontal areas.

We were able to unravel the temporal development of specific age-related dynamic network structures, which seem to be a necessary prerequisite for the execution of a motor act. The increased interhemispheric connectivity and the additional inclusion of frontal electrodes converge with but extend previous fMRI data, which report an overactivation, especially in the prefrontal and pre-motor areas, associated with a loss of hemispheric lateralization in OS. All observed network changes, i.e., an increase in frontal nodes and connections and the decrease in flexibility of the established large network, are compatible with a compensatory mechanism to maintain motor function in OS. We further hypothesize that the more extended information processing, suggested by a detour via frontal regions, is related to the longer reaction times observed in OS.

Keywords

Compensation, HAROLD, low frequencies, PASA, Phase locking

Introduction

Aging results in increased deficits in the execution and planning of movements, leading to delayed reactions and decreased movement accuracy (Wu and Hallett 2005; Seidler et al. 2010; Liu et al. 2017). Even though several studies investigated the effects of non-pathological aging on human motor performance, to date, our understanding of the neurobiological underpinnings of these changes remains sketchy.

Several fMRI studies reported an association between aging and changes in movement-related neural activity. In particular, a generally enhanced activation was reported, especially in pre-frontal and pre-motor areas (Sailer et al. 2000; Heuninckx et al. 2005; Ward et al. 2008). This effect is often referred to as the so-called PASA (posterior to anterior shift in aging) phenomenon (Dennis and Cabeza 2011). The HAROLD (hemispheric asymmetry reduction in older subjects) model proposes another effect often reported by fMRI studies, namely a reduced hemispheric asymmetry during cognitive processing, which is thought to be rather a general aging-associated than task-specific phenomenon (for a summary see (Cabeza 2002)). It is assumed that these effects (PASA and HAROLD) reflect either a compensatory mechanism, i.e., a recruitment of additional brain areas to support weakened functionality in core brain regions (Cabeza et al. 1997; Nolde et al. 1998; Reuter-Lorenz et al. 2000), or difficulties in recruiting specialized task-specific subnetworks in older subjects (Mitrushina and Satz 1991; Babcock et al. 1997; Cabeza 2002).

Up to now, the neural mechanisms underlying these changes in healthy aging remain elusive. One hypothesis states that they result from changes in inter-regional neural synchronization since this is a crucial mechanism underlying motor and cognitive tasks

(Fell et al. 2004; Popovych et al. 2016). Synchronization of distinct neural populations represents the organization of their temporally coordinated activities (for a review, see (Palva and Palva 2012)). Several studies using data from EEG/MEG/single-unit/ECog recordings while subjects performed a variety of different motor tasks showed that remote neural populations synchronize over a short-time period (Singer 1999; Singer 2004; Uhlhaas et al. 2010; van Wijk et al. 2012), suggesting that coordinated timing constitutes a fundamental principle involved in motor and cognitive processing (Baker et al. 1997; Baker et al. 2001; Fries 2005; Uhlhaas et al. 2010; Fries 2015).

In our previous study (Rosjat et al. 2018), we could show that during voluntary movements, motor-related networks built on inter-regional neural synchronization in younger as well as older subjects. In that study, we performed a phase-locking analysis between the neural signals recorded from the electrodes lying above the motor cortex with a low time resolution of 100 ms. In particular, we calculated the phase-locking value (PLV) between the electrodes of interest as it is a general characteristic for the quantification of synchronization between neural signals (Lachaux et al. 1999). The results of this previous study exhibited an increase in interhemispheric connectivity in older subjects compatible with the HAROLD model. Due to the restriction on electrodes above the motor cortex, we were unable to find evidence for the PASA phenomenon.

As the results mentioned above originate from fMRI studies or were analyzed without or only minor time resolution, little information is available about aging-effects on the contribution of different movement stages, i.e., stimulus processing, movement planning, and execution. Accordingly, we here aimed at investigating how changes related to healthy aging affect the organization of motor-related networks with a particular interest in the role

of prefrontal and premotor regions. Notably, we focused on connectivity patterns and their temporal evolution during different movement phases, as indexed by the phase relationship of distinct neural signals. For this reason, we used the high temporal resolution of the rPLV and applied it to Electroencephalography (EEG) data. The data were recorded from younger and older healthy participants who performed a simple visually-guided finger-tapping task to create a dynamic network based on phase relationships. A dynamic network (also dynamic graph) is a composition of temporally successive connectivity networks (or graphs) (Holme and Saramäki 2012; Sizemore and Bassett 2018). In contrast to static networks, dynamic networks take into account the temporal development of the connectivity. They, therefore, serve to provide a more precise temporal account of the different coupling structures of the respective age groups, especially about the influence of aging on the different movement phases.

Materials and Methods

Participants

In this study, we included EEG data of a group of twenty-one younger healthy individuals (10F/11M, age: 22-35 years) and of a group of thirty-one older healthy subjects (15F/16M, age: 60-78 years) first presented in two earlier studies (Popovych et al. 2016; Liu et al. 2017). All participants were right-handed according to the Edinburgh Handedness Inventory (Oldfield 1971) and had normal or corrected to normal color vision. The older participants had no history of psychiatric or neurological disease (as assessed by the Trail making test (TMT A: 41.16 ± 16.27 s, TMT B: 78.59 ± 28.02 s) (Spreen and Strauss 1998),

the Mini-mental-state-test (28.97 ± 1.29) (Folstein et al. 1975), the Clock-drawing test (Agrell and Dehlin 1998), and the Beck depression inventory (4.58 ± 3.21) (Beck et al. 1961)). All participants had given their written informed consent before the study. The local ethics committee of the Faculty of Medicine at the University of Cologne had approved both studies.

Experimental Design

We recorded EEG data while both groups performed a simple finger-tapping task. The experimental paradigm reported here consisted of two conditions, a motor condition (Fig. 1 (A)) and a vision-only control condition (Fig. 1 (B)). In the motor condition (visually-cued tapping, Fig. 1 (A)), the subjects were presented with a right- or left-pointing arrow (2° wide and 1.2° high, expressed as visual angles) for 200 ms on a screen with inter-stimulus intervals of varying length ≥ 4 s. The participants had to press a button with their left or right index finger, corresponding to the direction of the arrow, as fast as possible. In the second condition (vision-only, Fig. 1 (B)) the same stimuli as in the visually-cued tapping condition were presented. However, this time the participants were instructed to pay attention to the arrows but to refrain from performing or imagining to perform the button press. Thus, no motor action was performed in this condition (for full details see (Popovych et al. 2016; Liu et al. 2017)). During the experiment, a third, self-initiated tapping condition (not reported here) was recorded. In this condition, the participants were free to choose when to move which hand without any external stimuli (for details see (Wang et al. 2017)). The overall duration of the experiment, including breaks, was 70 min.

Our analyses were restricted to data acquired from the visually-cued and vision-only condition (Fig. 1 (A) and (B)), as it was necessary to use a contrast of the motor and control condition to reduce the contamination of the motor-related brain activity by the visual stimuli. Thus, the conditions had to be analyzed locked to the onset of the visual stimulus, which was not present in the self-initiated tapping condition.

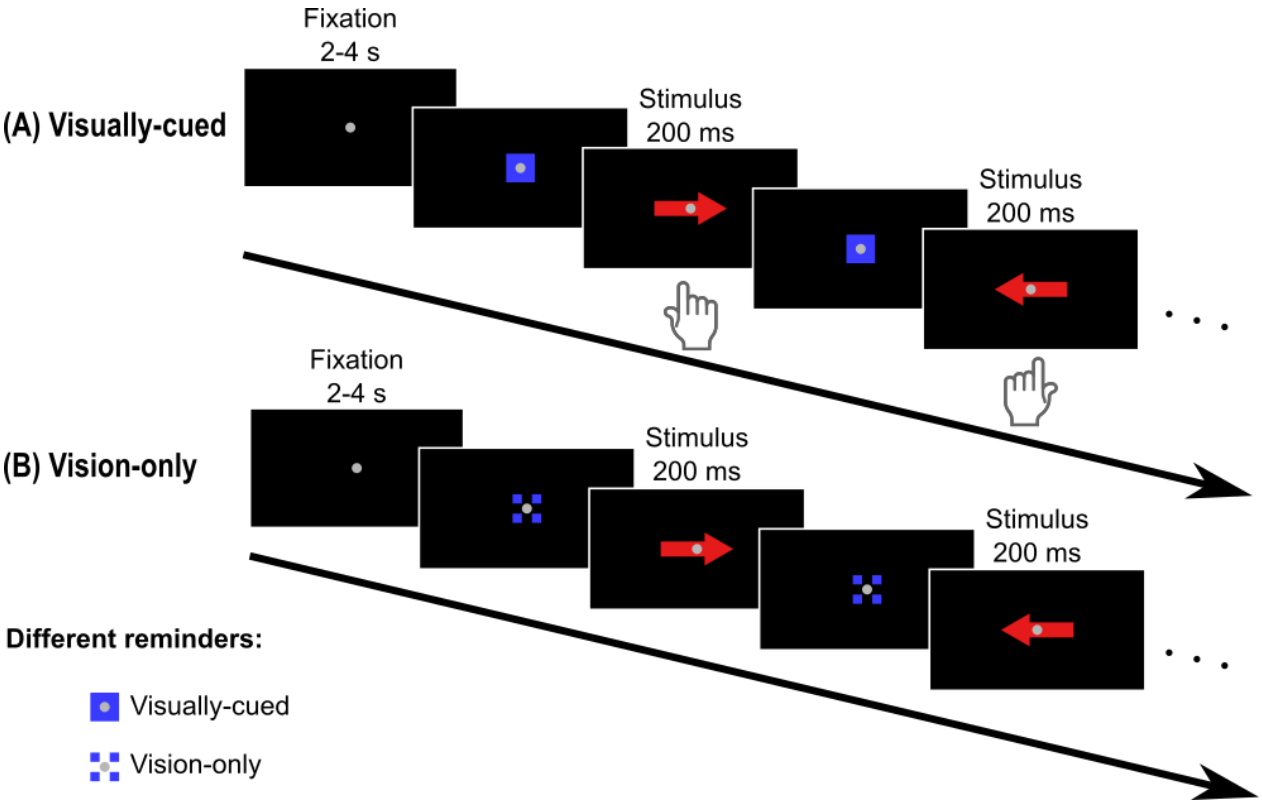

Fig 1. Experimental paradigm. *Organizational setup of the experiment. (A) Visually-cued finger movements and (B) vision-only condition. Each condition is represented by an unique reminder (e.g., a blue square in the visually-cued tapping condition). The arrows indicate the hand (left or right) to be used (adapted from Fig. 1 in (Wang et al. 2017)).*

EEG recording and preprocessing

While the subjects performed the task, we continuously collected EEG data from 64 active Ag/AgCl electrodes (Brain Products GmbH, Munich, Germany), placed according to the international 10-20 system. The reference electrode was placed at the left earlobe. Bipolar horizontal and left vertical electrooculograms (EOG) were recorded with three of the 64 scalp electrodes (previously located at FT9, FT10, and TP10 in the 10-20 system). These were placed at the bilateral outer canthi and under the left eye to monitor eye movements and blinking. Before the experiment, it was ensured that the impedances of all electrodes were below 15 $k\Omega$. The EEG signals were amplified, bandpass filtered in the frequency range $0.87 - 500$ Hz, and digitized at a sampling rate of 2.5 kHz. Index finger movement onsets were detected by acceleration sensors attached to the tip of each index finger. We also used the information from the acceleration signals to monitor the subjects' behavior, e.g., to rule out errors such as mirror movements. We defined the onset of the finger movement as the instant of time at which the numerical time derivative of the acceleration signal exceeded a predefined threshold.

The acquired raw data went through several offline pre-processing steps. First, we band-pass filtered the data from 0.5 to 48 Hz to remove slow voltage drifts. We next downsampled the data to 200 Hz to reduce the file size and thus the computing time. We then removed artifacts using a semi-automated process in EEGLAB using independent component analysis (ICA) (Makeig et al. 1996). Finally, the data were epoched to intervals $[-1500, +2500]$ ms, which centered around stimulus onset.

For our analysis, we excluded trials that contained EEG artifacts or included movements during the pre-stimulus period detected by the accelerometer. After excluding trials based on these criteria, we only considered data from participants who had at least 30 correct trials per hand. Based on these quality considerations, data from three younger and seven older subjects were excluded from further analysis. Thus, EEG data from 18 younger and 24 older subjects were used for further processing.

Spatial filtering

A crucial pre-processing step for the following connectivity analysis was spatial filtering. In the EEG, volume conduction is a primary concern in determining the relationship of signals. The activity of a single neural generator can influence the signal in several different electrode positions and thus lead to inaccurate phase-locking between these recording sites. To reduce the detection of false-positive connectivity, we applied spatial filtering using surface Laplacians, which demonstrably improves spatial resolution and allows the analysis of electrodes close to the region of interest (Lachaux et al. 1999). Thus, our preprocessed data were re-referenced to a small Laplacian reference to improve the spatial resolution of the signals and thus their suitability for subsequent connectivity analysis (Hjorth 1975).

Phase-locking analysis

Following preprocessing, we transformed the epoched and cleaned data to the time-frequency domain using Morlet wavelets (Kronland-Martinet et al. 1987) in a $\delta - \beta$ frequency range (2-30 Hz) with a step size of 1 Hz (5 cycles). This time-frequency decomposition was performed with the Statistical Parametric Mapping toolbox (SPM12,

Wellcome Trust Centre for Human Neuroimaging, London UK) implemented in MatLab R2018b (The MathWorks Inc., Massachusetts, USA). We then analyzed the phase information from the time-frequency decomposition using customized MATLAB scripts. The resulting networks were analyzed using graph theoretical metrics as implemented in the Brain Connectivity Toolbox (Rubinov and Sporns 2010).

We obtained the temporal evolution of the phase $\varphi(f,t)$ by applying the complex Morlet wavelet transformation for each frequency separately to our data. We quantified the communication of two different brain regions, i.e., acquisition sites, by synchronization determined by the single-frequency phase-locking value (sPLV; adapting the phase-locking value defined in (Lachaux et al. 1999)). For a pair of channels m and n, sPLV is defined as:

$$sPLV_{m,n}(f,t) = \frac{1}{N}\left|\sum_{k=1}^{N} \exp\left(i(\varphi_{m_k}(f,t) - \varphi_{n_k}(f,t))\right)\right|$$

here φ_{m_k} denotes the phase of the EEG at channel m in the k-th trial. N is the total number of trials, and i is the imaginary unit. While minimum sPLV $= 0$ represents a random distribution of phase differences over all trials without any coherence, a maximal sPLV $= 1$ occurs only in the case of perfect inter-trial phase locking of the phase differences between the EEG signals at the two channels m and n over all trials.

Since we were interested in an event-related measure that represented the synchronization increases and decreases during movement preparation and execution, we normalized the sPLV of the electrophysiological recordings at each pair of channels with respect to its baseline value and calculated its relative change over the entire epoch. We refer to these normalized sPLVs as *relative phase-locking values* (rPLVs):

$$rPLV_{m,n}(f,t) = \frac{sPLV_{m,n}(f,t) - \overline{sPLV_{m,n}(f)}}{\overline{sPLV_{m,n}(f)}}$$

here $\overline{sPLV_{m,n}(f)}$ denotes the sPLV of the baseline interval for each frequency, i.e., the mean sPLV at frequency f in the baseline interval, which was defined from $[-1300, -500]$ ms excluding the first 200 ms of the original interval as it contained edge artifacts of the Morlet transformation.

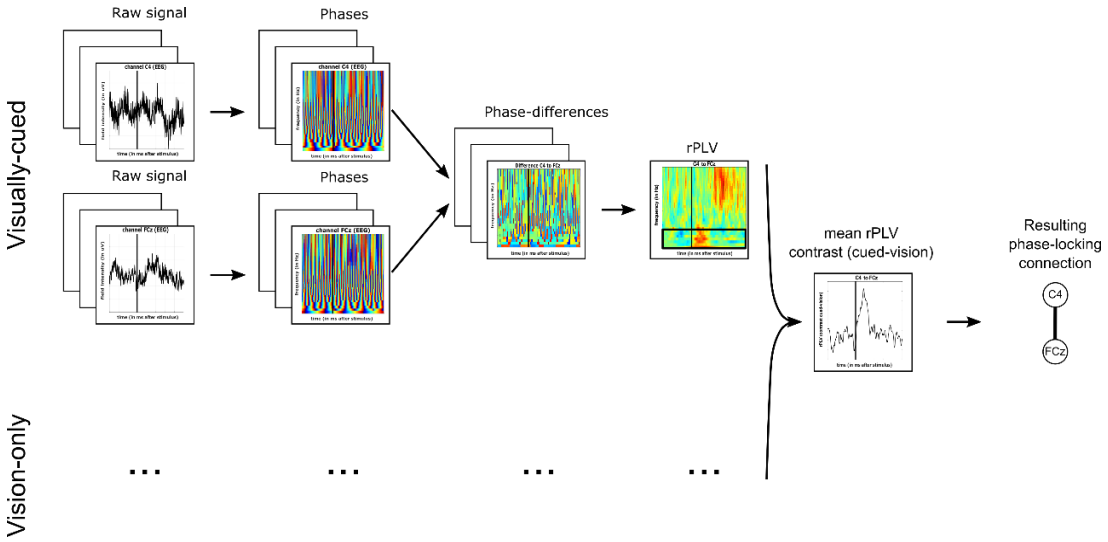

Fig 2. Phase-locking analysis. *Schematic illustration of the procedure to construct corresponding phase-locking networks from contrasted, i.e., visually-cued - vision-only, rPLVs (adapted from Fig. 1 in (Rosjat et al. 2018)). The black vertical lines represent movement onset.*

To analyze inter-regional synchronization, we considered four major frequency bands: δ (2-3 Hz), θ (4-7 Hz), α (8-12 Hz), and β (13-30 Hz). Instead of first filtering the signal to a specific frequency band, we calculated the rPLV separately for each frequency with a resolution of 1 Hz before averaging these values over the frequencies of the frequency band. In this way, we ensured a true 1:1 frequency coupling that maximizes the contribution of

each frequency in the band. The steps described above were performed for both the tapping and the vision-only control condition. The resulting mean rPLVs (averaged over a frequency band of interest) were then contrasted by subtracting the vision-only control condition from the visually-cued condition, resulting in positive values when phase-locking is stronger in visually-cued and negative values for stronger phase-locking in the control condition. (cf. Fig. 2). The contrasted mean rPLVs then underwent statistical testing (described below) to define the edges of the phase-locking network.

Statistical analysis

To test whether the difference between the mean rPLV (averaged over the frequency band) and the baseline (averaged over the frequency band) was statistically significant, we compared the mean rPLV obtained for each pair of electrodes at each time point in the interval [0,1000] ms with its baseline value. To this end, we used a pointwise t-test with a significance level of $p < 0.05$, corrected for multiple comparisons (false discovery rate, FDR, $q = 0.05$) (Benjamini and Hochberg 1995). The correction was performed concerning the number of time points, age groups, and electrodes. The baseline was constructed by generating normally-distributed random values that had the same mean and standard deviation as the EEG at any time point of the baseline interval $[-1300, -500]$ ms. For the construction of the rPLV networks, we defined a *connection*, i.e., an edge of the network, between two given nodes to exist at a given time point t if the mean rPLV between these two nodes was significantly increased with respect to its baseline value. Based on our previous results (Popovych et al. 2016; Rosjat et al. 2018), which showed a symmetrical behavior of phase-locking, and to reduce the number of statistical comparisons, the rPLVs during left- and right-hand finger movements were collapsed together after flipping the

ones for the right-hand movements. Electrodes were defined as being either ipsilateral or contralateral to the moved hand. For convenience, results are presented resembling left-hand movements, i.e., electrodes over the left hemisphere are assumed to be ipsilateral while electrodes over the right hemisphere are assumed to be contralateral of the performed movement.

Dynamic network analysis

The statistical analysis above defines a binary undirected graph $G_t = (V, E_t)$, where the graph G is defined by a set of vertices V and edges $E_t: V \times V \rightarrow$ R, for each point in time t for younger and older participants. The dynamic graph, also called temporal network, is defined as the ordered set of graphs $G(t) = \{G_t | t \in [1, \ldots, T]\}$. It can also more efficiently be represented by a list of triples (i, j, t), defining the contacts of two nodes i and j and the time point t at which they occur (Sizemore and Bassett 2018). In contrast to static graphs, dynamic graphs account for time-varying connectivity patterns that might reflect the formation of subnetworks due to task performance.

Besides to the time-varying networks, we investigated the *aggregated graph* of the dynamic network, which is a graph that accounts for the number of occurrences of each edge over all graphs, i.e., edges that appear more often have a higher weight while rarely present edges have a smaller weight. We performed a cluster analysis using the Louvain community algorithm, which uses a greedy optimization method to minimize the ratio of the number of edges inside communities to edges outside communities, for each time step and the aggregated graph for both groups of participants to retrieve information on closely connected subnetworks (Reichardt and Bornholdt 2006; Blondel et al. 2008; Ronhovde and

Nussinov 2009; Sun et al. 2009). To reduce the effect of randomly assigned cluster labels between time points, we always used the previous cluster as the initial condition for the following community detection. Additionally, we post-hoc assigned the label for each community, minimizing the number of label switches between time points, which prevents the same cluster from being assigned different cluster labels at consecutive time points. Furthermore, based on these clusters we tested the similarity of clusters between age groups by computing the variation of information (VI) (Meilă 2007)

$$VI(X,Y) = \frac{H(X) + H(Y) - 2MI(X,Y)}{\log(n)}$$

where H is entropy, MI is mutual information, and n is the number of nodes. This metric ranges from 0, i.e., identical clustering, to 1 (as it is normalized by $\log(n)$), i.e., maximally distinct clustering. To account for actual age effects, we compared $VI(X,Y)$ (X representing YS and Y representing OS) with time-lagged self-distribution distances $VI(X(t),X(t-1))$ and $VI(Y(t),Y(t-1))$ to test whether the partition distance between younger and older subjects is larger than within-group partition changes in time.

The flexibility F of the dynamic network is defined by the average of all *node flexibilities* f_i (Bassett et al. 2011), which are defined as the number of times that a node changed communities, normalized by the maximal number of times this node could have changed communities,

$$f_i = \frac{m}{T-1}$$

with m the number of community changes and T the number of time points.

Finally, we analyzed the hub nodes of the networks. Those nodes play a crucial role in the network, as they serve as the connection between different subnetworks. For the analysis of hub nodes, we calculated the *betweenness centrality* for each time point, which is defined as the fraction of shortest paths that pass through each node (Brandes 2001; Kintali 2008). We primarily focused on the first occurrence of each hub node in the network.

Results

Behavioral results

We first tested whether there was a significant difference between older subjects (OS) and younger subjects (YS) in reaction times (RT), defined as the time that elapsed from stimulus presentation until movement onset, and accuracy rate, i.e., the percentage of correct responses among all trials. The reaction time was significantly longer in older subjects ($497\,\text{ms} \pm 84\,\text{ms}$) than in younger subjects ($426\,\text{ms} \pm 77\,\text{ms}$), $t(82) = 3.9442, p < 0.0001$. The mean response accuracy in the visually-cued condition for older subjects ($93.13\% \pm 5.69\%$) and younger subjects ($97.7\% \pm 2.22\%$) was greater than 90%, consistent with the instructions. However, as expected, the accuracy was lower for the older participants, $t(40) = -3.2329, p = 0.0025$. In summary, we found an age-related deceleration and reduced accuracy in motor task performance.

Event-related increase in phase-locking

We analyzed visually-cued index finger movements of the left and right hand in relation to the onset of the visual stimulus. Since we were interested in the phase-locking related to the motor performance, we computed the contrast of the motor (visually-cued) and the control

condition (vision-only) to reduce the influence of visual stimulation. We found an increased phase-locking in the $\delta - \theta$ frequency band (2-7 Hz) during movement execution and in the β frequency band (13-30 Hz) in the post-movement period (approx. 500 ms after stimulus presentation). Since we were interested in the evolution of the dynamic graphs during the execution of the motor act and due to the results of our earlier studies (Popovych et al. 2016; Rosjat et al. 2018), we hence focused our further dynamical graph analysis on the $\delta - \theta$ frequencies.

Dynamic motor network analysis

Time-varying network analysis

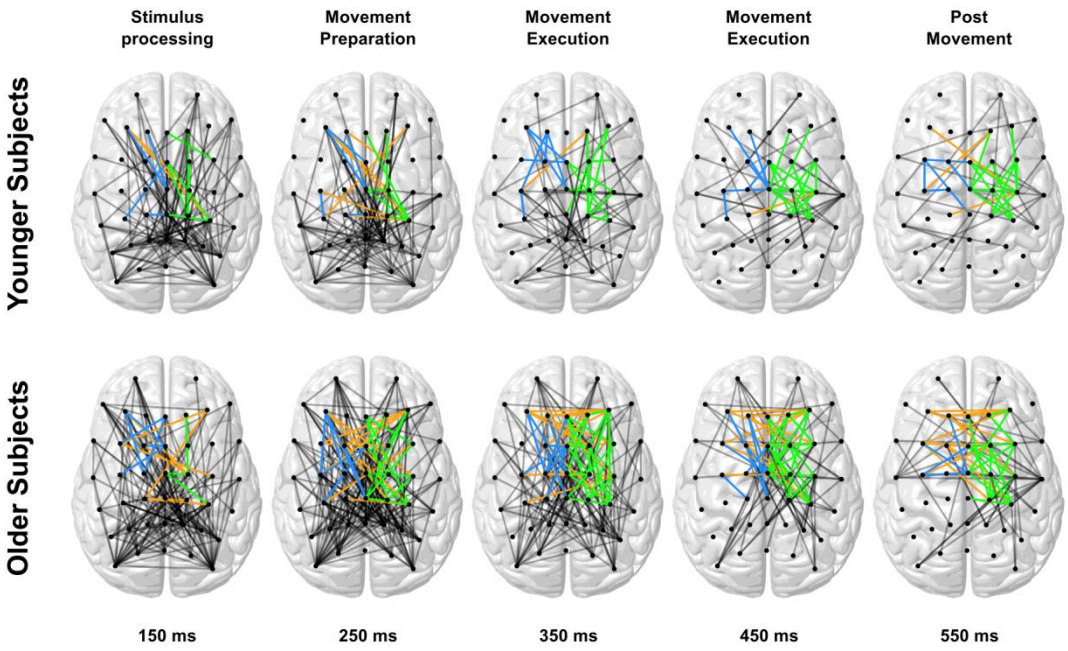

Fig 3. Dynamic graph snapshots. *Exemplary graph snapshots for YS (top) and OS (bottom) for five different time points representative for stimulus processing, movement preparation, execution, and post movement. Edges related to the core motor network are color-coded in*

blue (ipsilateral), green (contralateral), and orange (interhemispheric). Color codes are chosen as in (Rosjat et al. 2018) for better comparison.

Phase-locking in the $\delta - \theta$ frequency band was used to construct connectivity matrices for each time point of the trial, which resulted in a dynamic graph (see Materials and methods - *Dynamic network analysis*). Representative networks are shown in Fig. 3. The figure displays network connectivity, which can roughly be assigned to stimulus processing (150 ms), movement preparation (250 ms), movement execution (350 & 450 ms), and the post movement phase (550 ms). The younger subjects displayed the densest networks in the stimulus processing and movement preparation phase, the older subjects additionally in the early phase of movement execution. The connections in YS networks clustered around occipital regions and central motor-related regions, while OS networks showed a dense connectivity spread over the whole brain. Both group of subjects associated graphs expressed pronounced connectivity between ipsilateral (blue) and contralateral (green) sensorimotor nodes in the movement execution and post movement phase. The older subjects' networks, however, additionally included an increased number of interhemispheric connections (orange), which were already present in the movement preparation phase. Overall, older subjects' networks displayed an increase in connectivity, leading to a denser graph.

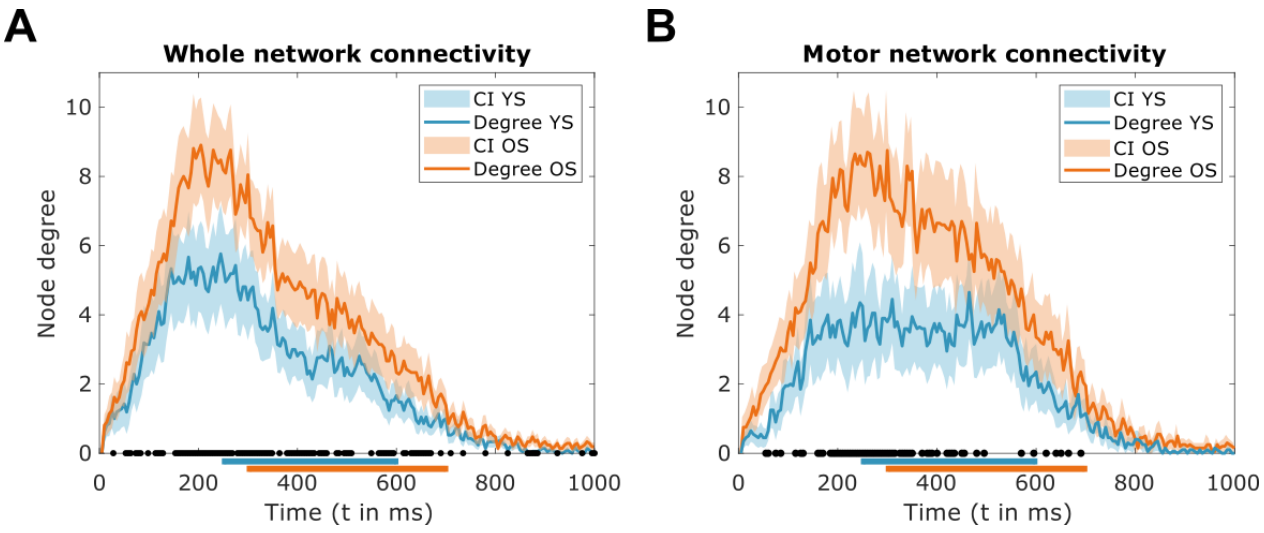

Fig 4. Node degree dynamics. *A: Timecourses of the average overall node degrees of YS (blue) and OS (red) surrounded by shaded regions representing the confidence interval. B: Timecourses of the average motor network node degrees of YS (blue) and OS (red) surrounded by shaded regions representing the confidence interval. Movement periods are marked with blue (YS) and red (OS) solid lines at the x-axes. Intervals with significant differences between age groups are marked with black dots.*

We quantified this by analyzing the average node degree over time for YS and OS (Fig. 4). A paired t-test showed that the average node degree was significantly increased in OS compared to YS in whole network connectivity, i.e., taking all nodes of the network into account, t's< -2.9027, p's < 0.05 (FDR-corrected), df $= 60$, $0.3404 \leq$ sd's ≤ 4.7489. The same effect was observed about motor network connectivity, i.e., taking only nodes above the motor-related regions into account, t's < -3.3773, p's < 0.05 (FDR-corrected), df $= 19$, $1.0954 \leq$ sd's ≤ 4.8284. In both cases, the significant differences were mainly present in the time interval from 200 to 400 ms.

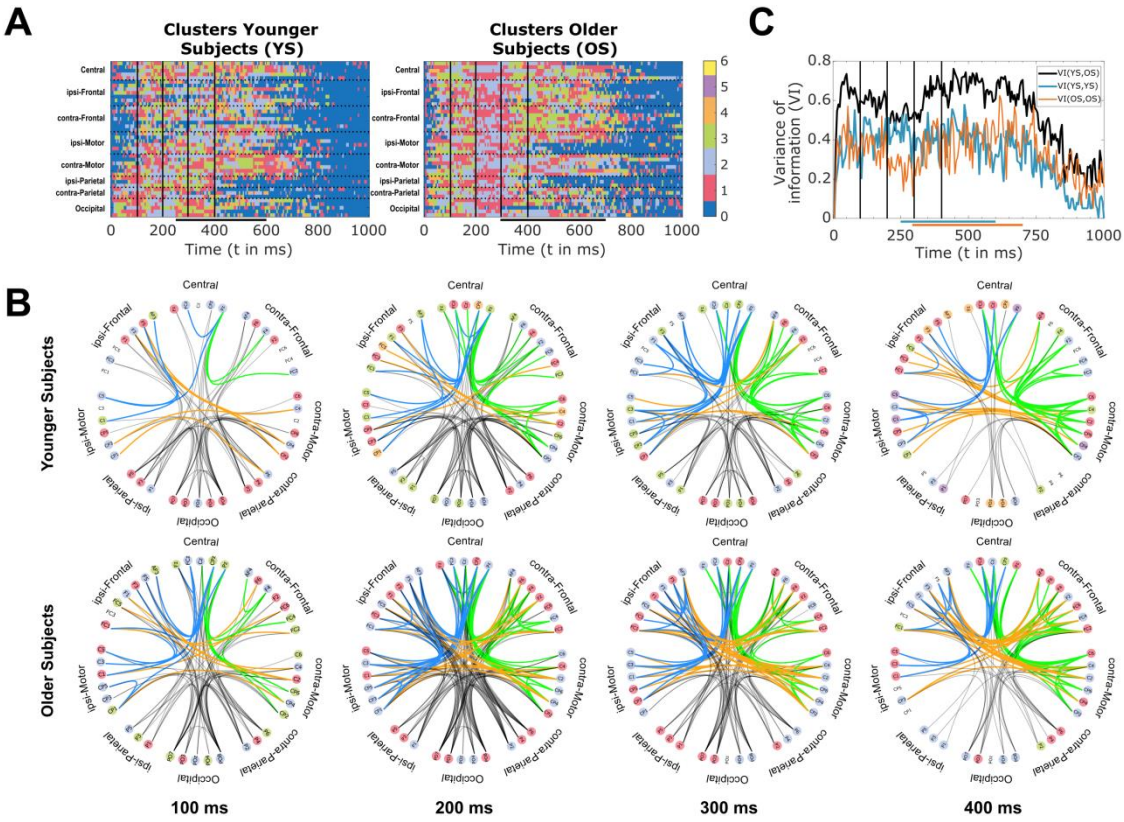

Fig 5. Louvain clustering. *A: Channel partitions for YS (left) and OS (right). Clusters are labeled from 1 to 6 (with arbitrary colors). Unconnected channels are displayed in blue (cluster 0). Movement periods are marked with black horizontal lines. B: Circular graphs showing representative clusterings from 100 ms, 200 ms, 300 ms, and 400 ms post stimulus. Nodes are colored corresponding to the clusters in A. Edges related to the core motor network are color-coded in blue (ipsilateral), green (contralateral), and orange (interhemispheric). C: Distribution distance for clusters computed for younger and older subjects (black) compared to self-distribution distances of younger (blue) and older subjects (red). Movement periods are marked with blue (YS) and red (OS) solid lines.*

In the following, we applied the Louvain clustering method (clustering parameter $q = 0.9$), which measures the density of edges inside communities to edges outside communities to

separate the graphs into sets of closely interconnected subnetworks (Fig. 5 A, B). During stimulus processing, YS networks were separated in a cluster with a focus on occipital and parietal electrodes (red nodes) and a cluster containing motor, frontal, and central electrodes (light blue nodes). OS networks, on the other hand, were divided into three more widespread clusters with electrodes from almost all eight regions (Fig. 5 B (100 ms)). In the movement preparatory and early movement execution phases (200-300 ms), OS network clusters were reduced to two extended, stable clusters that integrated electrodes from all 8 regions (cf. Fig. 5 B (200 and 300 ms)). The YS networks, on the other hand, broke up into several smaller clusters, also showing no clear regional distinction. A paired t-test showed a significant reduction in node flexibility in OS, t(40) = 5.6589, $p < 0.001$, $\Delta_{\overline{f_y}-\overline{f_o}} = 0.1742 \pm 0.0622$, in the interval (200, 300) ms. Even when the interval was increased to (1-700) ms the node flexibility was significantly reduced in OS, t(40) = 2.7318, $p = 0.00925$, $\Delta_{\overline{f_y}-\overline{f_o}} = 0.0426 \pm 0.0315$. During movement execution the number of connections decreased (cf. Fig. 4 A), which led to a sparser network that for YS could be divided mainly into a contralateral motor - central - ipsilateral frontal community (red) and several smaller communities (Fig. 5 B, 400 ms). In OS, the motor, frontal, and central electrodes were more densely connected, which led to less distinct clusters as in YS.

We calculated the variance of information (VI), which serves as a marker of the difference of two clusters of the same nodes, between both groups for each time point (VI(YS,OS)). As a comparison and, in particular, to detect real effects of age, we calculated the VI for YS (VI(YS,YS)) and OS (VI(OS,OS)) for consecutive time points (Fig 5 C). With this analysis, we could show that the variance between age groups stays at a high level in the first 700 ms of the epoch (with a value between 0.6-0.8). The variance between age groups was constantly

higher compared to the self-distribution distances of YS and OS, except for the time interval [200, 300] ms. In this interval, the self variance of information for OS displayed a drop, which was related to the less variable networks, i.e., the decreased node flexibility during movement preparation described above. At the same time, YS showed an increased variance of information reflecting a high clustering variability during that time.

Aggregated networks

In the following, we investigated the aggregated networks, i.e., the sum of all unweighted connectivity matrices over all time points t, for YS and OS. The resulting networks are presented in Fig. 6. YS and OS showed densely connected nodes above the occipital cortex, which were related to the early time intervals of the dynamic graphs. In YS the motor network showed additionally dense connectivity between nodes above ipsilateral frontal and central regions (blue), diagonal interhemispheric connections between nodes above the ipsilateral frontal and contralateral motor cortex (orange), horizontal interhemispheric connections between nodes above the ipsilateral and contralateral motor cortex (orange), and between nodes above the contralateral motor and central electrodes (green) (Fig. 6 A). In contrast, OS showed a densely connected network between all nodes (cf. Fig. 4), but more strikingly an increase in interhemispheric horizontal connectivity between nodes above the frontal, frontocentral, and central regions, i.e., between nodes above the ipsilateral and contralateral frontal and above the ipsilateral and contralateral motor cortex (Fig. 6 B).

Additionally, we investigated the Louvain clustering for the aggregated networks (Fig. 6 C and D). Both aggregated networks could be clustered into three communities, which are represented by different colored nodes in (blue, red, and green). The YS network clustered

into an occipital-parietal cluster (red nodes), a cluster mainly involving the nodes above the ipsilateral frontal, central, and contralateral motor cortex (blue nodes) and a contralateral frontal and ispilateral motor regions one (green), whereas the OS network showed a cluster that mainly involved nodes above frontal areas and ipsi- and contralateral motor cortex (blue nodes), a cluster above parietal and central areas (green nodes), and one cluster containing the remaining nodes (red). Thereby, the clustering results of the aggregated networks supported the network differences of the dynamic networks during movement execution described above.

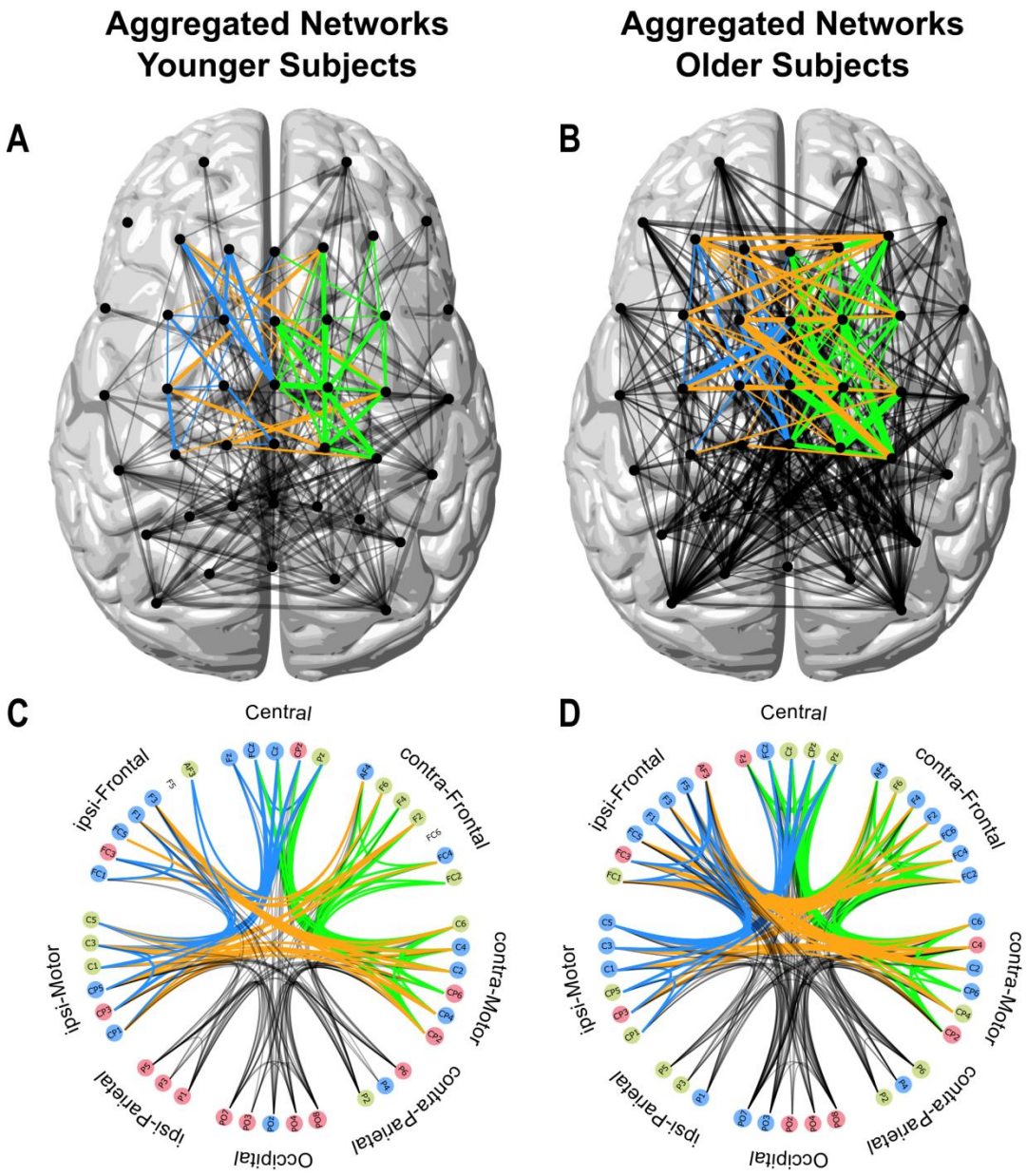

Fig 6. Aggregated networks in aging. *Top: Representation of the aggregated networks for younger (A) and older subjects (B). The thickness of the lines accounts for the number of occurrences of the corresponding edge in the respective time interval. Bottom: Circular representation of the aggregated networks for younger (C) and older subjects (D). Nodes are color-coded depending on assigned clusters. Edges related to the core motor network are color-coded in blue (ipsilateral), green (contralateral), and orange (interhemispheric).*

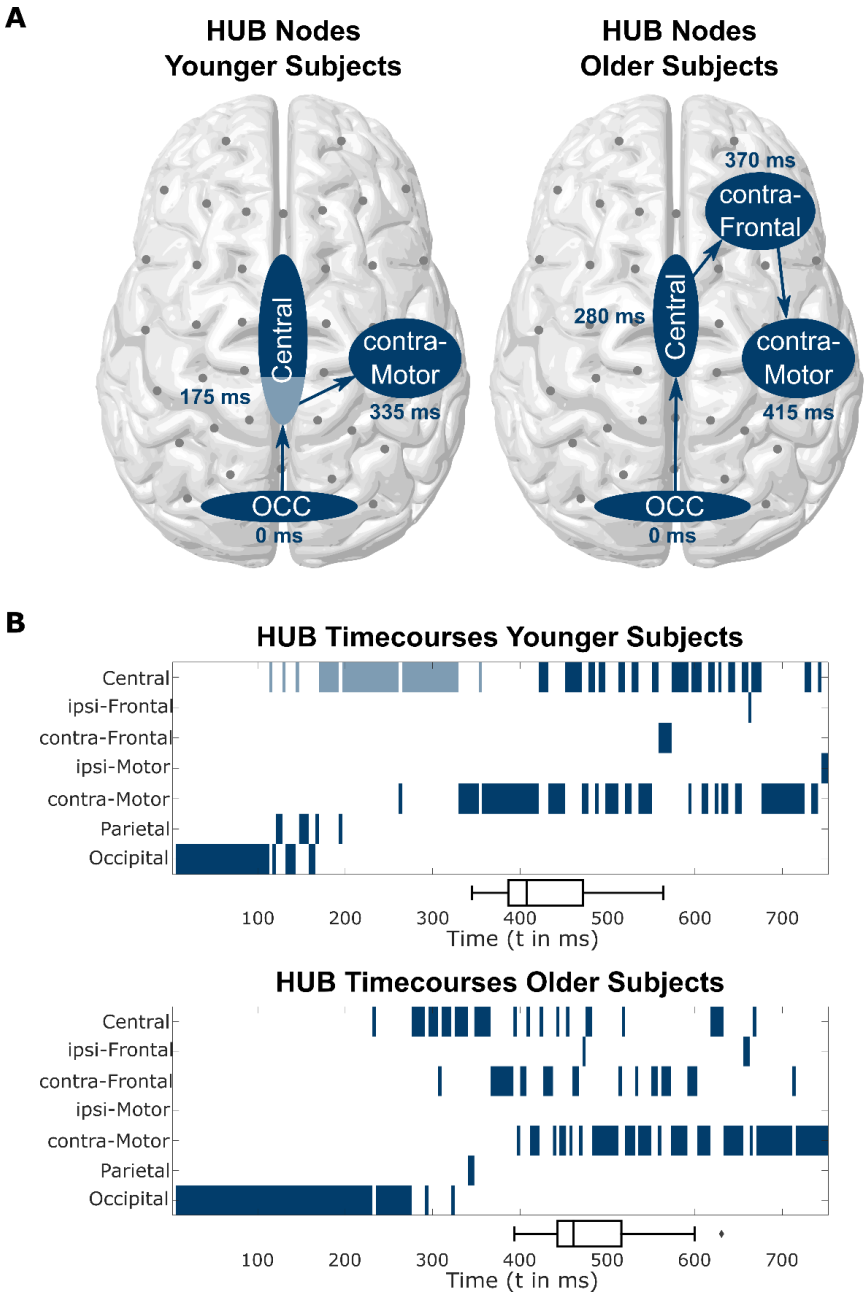

Fig 7. HUB nodes. *Timepoints of first occurrences of HUB nodes (A) and timecourses of HUB nodes in the interval [0, 750] ms (B) - represented by groups of electrodes (Occipital: PO7, PO8; Central: Pz (light blue), CPz, Cz, FCz; contra-Frontal: FC2, FC4, FC6, F2, F4, F6; contra-Motor: C2, C4, C6, CP2, CP4, CP6) - as defined by betweenness centrality in the networks of younger and older subjects. The mean reaction times for each age group are depicted by boxplots on the x-axis.*

HUB node analysis

In the last step, we analyzed the HUB nodes of the dynamical graphs using the betweenness centrality. We investigated the order of first appearance as well as the timecourse of the HUB nodes (Fig. 7). In both groups, occipital nodes appeared as the first HUB nodes in the system. In YS, HUB nodes were then shifted to parieto-central (light blue) and later to contralateral motor nodes. After most participants pressed the button (cf. Fig. 7: B (boxplot)), the HUB nodes switched back and forth between central/fronto-central (dark blue) and contralateral motor nodes. Whereas OS HUB nodes first shifted to central and fronto-central nodes, from there to contralateral frontal nodes, and only in the last step to contralateral motor nodes. A comparison of the timecourses showed that OS HUBs remained roughly 100 ms longer in occipital nodes than in YS. Thus, YS HUB nodes shifted about 100 ms earlier to parieto-central nodes and finally also to contralateral motor nodes.

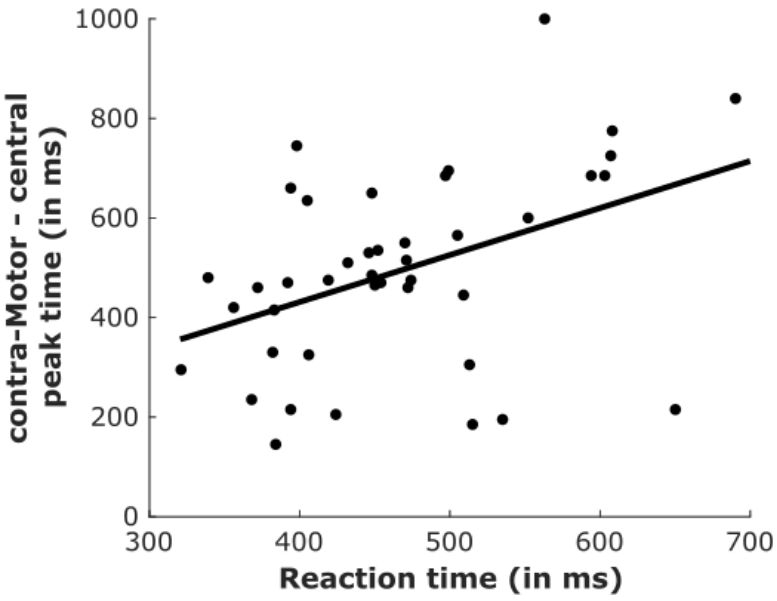

Fig 8. Behavioral correlation *Each subject's reaction time (both age groups) plotted against the rPLV peak time between virtual contralateral motor and central electrodes.*

Because of the results presented in Fig. 7, we hypothesized that the timing of connectivity between electrodes above contralateral motor and central regions might be a crucial factor in establishing the differences in behavioral output observed between OS and YS. For this, we investigated whether the peak time of the rPLV was related to the timing of movement output, i.e., the reaction times. Since rPLV was strongest either between C4 and Cz/FCz or CP4 and Cz/FCz, we decided to create a virtual connection by averaging over all four possible combinations. The reaction time was significantly correlated to this virtual contralateral motor-central connection, $p < 0.01, \rho = 0.42$ (see Fig. 8).

Discussion

We performed a dynamic graph analysis on EEG data recorded from healthy younger and older participants, while they performed a visually-cued finger-tapping task. The graphs were based on phase-locking as a measure of inter-regional synchronization, which, according to the communication through coherence (CTC) hypothesis, reflects increased functional connectivity between neural populations expressed by coherently coordinated firing patterns (Fries 2005, 2015). For this purpose, we calculated the rPLV, which measures the instantaneous synchronization between two distinct recording sites. The great advantage of rPLV is that it is capable of measuring fast transient synchronizations and thus preserves the advantage of the high temporal resolution of EEG recordings, which is essential for the construction of dynamic graphs related to the motor task. In contrast, other frequently used methods like dynamic causal modeling (DCM) or Granger causality require statistically stationary signals and thus result in connectivity information with lower time resolution. Since some of the effects we observed (e.g., decreased node

flexibility) lasted for only a few hundred milliseconds and, hence, could not guarantee stationary signals (as they took place close to the button press), the application of rPLV instead of DCM or Granger causality was crucial for investigating the underlying dynamic neural networks in our study.

To start with, we computed the rPLVs between all pairs of the considered electrodes in the $\delta - \theta$ frequency range. The electrodes were then defined as the nodes of the dynamic graph, while the edges for each time-point represented significantly increased rPLVs. We compared the time evolution of the dynamic networks that we obtained for the younger and older subjects with a focus on movement preparation and movement execution. We investigated the networks considering three different aspects: the overall connectivity, i.e., the node degree of the whole graph in general and the one of the motor-related nodes, the formation of clusters, i.e., subnetworks during the different movement phases, and the evolution of HUB nodes over time.

Setup of dynamic networks

In the construction of the dynamic network, we defined a connection at a given time point to be present if the respective rPLV was significantly increased compared to baseline (i.e., before the stimulus) levels. Since this involved extensive testing, we applied FDR correction (q = 0.05) to account for the considerable number of multiple comparisons. One could argue that this method is not strict enough. However, it has turned out that even with a stricter FDR correction (q = 0.01), the main differences in motor-related networks between YS and OS prevailed and the core message of our results remained unaffected (results not shown). Furthermore, we decided to analyze our data at the electrode level. At least in principle, a

source localization could have provided further insights into the origin of the effects reported here. However, we refrained from doing so to avoid the ill-posed inverse problem, which only provides an assumption of the source activity and could, therefore, lead to erroneous interpretations (Grech et al. 2008; Wendel et al. 2009; Bradley et al. 2016). Instead, we used the small Laplacian reference to substantially reduce the effect of volume conduction on our data (Lachaux et al. 1999). Although not a source localization method, through the small Laplacian, electrodes that are directly above the sources are maximally sensitive to the underlying activity.

Dynamic graph connection density

Several fMRI studies have reported an overactivation related to the aging human brain (Sailer et al. 2000; Heuninckx et al. 2005 et al. 2008; Dennis and Cabeza 2011). In our earlier study (Liu et al. 2017), we found a decreased (more negative) event-related desynchronization in the α and β frequencies in motor-related electrodes in older subjects. There, we did not find any general overactivation over a large number of electrodes in any frequency band, especially not in the $\delta - \theta$ frequency band, as we report here. The results reported here revealed a general increase in node degree in all electrodes during movement preparation and execution (Fig. 4 A). Especially in motor-related electrodes, YS showed a plateau-like behavior while OS node degree showed a peak roughly twice as high during movement preparation (Fig. 4 B). This effect might reflect *over-connectivity*, which may relate to the overactivation previously reported in fMRI studies.

Community structure

The analysis of the aggregated networks revealed a substantial increase in the number of interhemispheric connections in OS. The cluster analysis of aggregated networks in YS unraveled three clusters, a cluster mainly consisting of parietal and occipital electrodes, a cluster of ipsilateral frontal, central, and contralateral motor electrodes, and a cluster that included ipsilateral motor and contralateral frontal electrodes. In OS, on the other hand, there was no clear separation in clusters possible. This might be related to the increased number of interhemispheric connections and thus a weaker inter-regional separability, which is consistent with the HAROLD model stating reduced hemispheric asymmetry during cognitive tasks (Cabeza 2002).

Additionally, we performed a similar cluster analysis on the dynamical graphs for each time-point. The clusters were different in both groups for almost the whole analyzed period (Fig. 5 B,C). The dynamic graph communities in YS during motor execution were, similar to the aggregated ones described above, separated in a more structured way, i.e., a dominant cluster including ipsilateral frontal, central, and contralateral motor electrodes, (cf. Fig. 5 B). The most striking difference between YS and OS was observed during movement preparation, i.e., immediately before movement onset. While YS showed a peak in VI between time-points in this epoch, i.e., a very variable network structure, OS networks exhibited a dip in VI (cf. Fig. 5 A, C in [200-300]ms). This visual inspection was confirmed by an analysis of node flexibility, which revealed a significant decrease in node flexibility in OS in that time interval. The decreased flexibility in OS networks might be related to the *over-connectivity* described above and the fact that OS expressed difficulties in recruiting

task-specific subnetworks and needed the whole network, i.e., higher effort to keep nearly the same task performance as YS.

Network information flow

We furthermore included an analysis of HUB nodes of the dynamical graphs, i.e., nodes connecting different clusters by a large number of connections. Here, we focused on the first occurrence and the timecourses of HUB nodes as one of the key players in the network. In YS, the networks involved a direct shift of the HUB nodes from occipital via parieto-central to contralateral sensorimotor electrodes. Once YS had executed the movement, HUB nodes switched back and forth between central and contralateral motor electrodes, which might be related to the incoming sensory feedback from the button press. The networks of OS, in contrast, shifted from occipital to central/fronto-central electrodes and then targeted an additional HUB node above contralateral frontal electrodes, which appeared at 370 ms, i.e., approximately the same time as the shift to contralateral motor areas in YS. Finally, the connectivity to contralateral sensorimotor areas dominated, which occurred roughly 80 ms later than in YS (Fig. 7). This shift of the HUB nodes to more frontal areas is compatible with the PASA (posterior-anterior shift in aging) phenomenon (Dennis and Cabeza 2011), which refers to the fact that the overall activity in OS is shifted to more frontal areas representing a stronger involvement of cognitive control. We hypothesize that this *detour* via frontal areas is accountable for longer reaction times in OS. This hypothesis is supported by the reported positive correlation between the reaction times and the peak timing of the connection between central and contralateral motor electrodes (Fig. 8).

Motor network connectivity during voluntary movements

In a previous publication (Rosjat et al. 2018), we reported on an invariant, i.e. present and unchanged in all movement phases, motor network in younger volunteers consisting of iPFC/iPM, mPFC/SMA, and cSM. This invariant network was significantly attenuated in OS and accompanied by increased interhemispheric connectivity. The results we have presented here reveal comparable patterns. YS established most (motor-related) connections between ipsilateral frontal, central, and contralateral motor regions (cf. aggregated networks in Fig. 6 A and dynamic networks during motor execution in Fig. 5 B). The networks of OS, on the other hand, showed additional interhemispheric connections, especially between ipsilateral frontal and contralateral frontal as well as ipsilateral motor and contralateral motor electrodes. Also, similar to the results during voluntary movements, OS exhibited higher connectivity between central and contralateral frontal electrodes. These results indicate that by investigating the contrast between visually-cued and vision-only conditions, we devised a condition alike the pure motor task (voluntary movement). Furthermore, these findings indicate that we identified a highly stable core network (iPFC/iPM - mPFC/SMA - cSM) that is important for movement execution over several experimental conditions.

Acknowledgements

This study was funded by the University of Cologne Emerging Groups Initiative (CONNECT) within the framework of the Institutional Strategy of the University of Cologne and the German Excellence Initiative. SD gratefully acknowledges additional support from the

German Research Foundation, Germany (DA1953/5-2). GRF gratefully acknowledges additional support from the Marga and Walter Boll Foundation.

References

Agrell, Berit, and Ove Dehlin. 1998. "The clock-drawing test." *Age and Ageing* 27 (3): 399–403. https://doi.org/10.1093/ageing/27.3.399.

Babcock, Renée L, Kerrie D Laguna, and Scott C Roesch. 1997. "A Comparison of the Factor Structure of Processing Speed for Younger and Older Adults: Testing the Assumption of Measurement Equivalence Across Age Groups." *Psychology and Aging* 12 (2). American Psychological Association: 268.

Baker, SN, Etienne Olivier, and RN Lemon. 1997. "Coherent Oscillations in Monkey Motor Cortex and Hand Muscle Emg Show Task-Dependent Modulation." *The Journal of Physiology* 501 (1). Wiley Online Library: 225–41.

Baker, SN, R Spinks, A Jackson, and RN Lemon. 2001. "Synchronization in Monkey Motor Cortex During a Precision Grip Task. I. Task-Dependent Modulation in Single-Unit Synchrony." *Journal of Neurophysiology* 85 (2). American Physiological Society Bethesda, MD: 869–85.

Bassett, Danielle S, Nicholas F Wymbs, Mason A Porter, Peter J Mucha, Jean M Carlson, and Scott T Grafton. 2011. "Dynamic Reconfiguration of Human Brain Networks During Learning." *Proceedings of the National Academy of Sciences* 108 (18). National Acad Sciences: 7641–6.

Beck, Aaron T, Calvin H Ward, Mock Mendelson, Jeremiah Mock, and John Erbaugh. 1961. "An Inventory for Measuring Depression." *Archives of General Psychiatry* 4 (6). American Medical Association: 561–71.

Benjamini, Yoav, and Yosef Hochberg. 1995. "Controlling the False Discovery Rate: A Practical and Powerful Approach to Multiple Testing." *Journal of the Royal Statistical Society: Series B (Methodological)* 57 (1). Wiley Online Library: 289–300.

Blondel, Vincent D, Jean-Loup Guillaume, Renaud Lambiotte, and Etienne Lefebvre. 2008. "Fast Unfolding of Communities in Large Networks." *Journal of Statistical Mechanics: Theory and Experiment* 2008 (10). IOP Publishing: P10008.

Bradley, Allison, Jun Yao, Jules Dewald, and Claus-Peter Richter. 2016. "Evaluation of Electroencephalography Source Localization Algorithms with Multiple Cortical Sources." *PloS One* 11 (1). Public Library of Science: e0147266.

Brandes, Ulrik. 2001. "A Faster Algorithm for Betweenness Centrality." *Journal of Mathematical Sociology* 25 (2). Taylor & Francis: 163–77.

Cabeza, Roberto. 2002. "Hemispheric Asymmetry Reduction in Older Adults: The Harold Model." *Psychology and Aging* 17 (1). American Psychological Association: 85.

Cabeza, Roberto, Cheryl L Grady, Lars Nyberg, Anthony R McIntosh, Endel Tulving, Shitij Kapur, Janine M Jennings, Sylvain Houle, and Fergus IM Craik. 1997. "Age-Related Differences in Neural Activity During Memory Encoding and Retrieval: A Positron Emission Tomography Study." *Journal of Neuroscience* 17 (1). Soc Neuroscience: 391–400.

Dennis, Nancy A, and Roberto Cabeza. 2011. "Neuroimaging of Healthy Cognitive Aging." In *The Handbook of Aging and Cognition*, 10–63. Psychology Press.

Fell, Juergen, Thomas Dietl, Thomas Grunwald, Martin Kurthen, Peter Klaver, Peter Trautner, Carlo Schaller, Christian E Elger, and Guillén Fernández. 2004. "Neural Bases of Cognitive Erps: More Than Phase Reset." *Journal of Cognitive Neuroscience* 16 (9). MIT Press: 1595–1604.

Folstein, Marshal F, Susan E Folstein, and Paul R McHugh. 1975. "'Mini-Mental State': A Practical Method for Grading the Cognitive State of Patients for the Clinician." *Journal of Psychiatric Research* 12 (3). Pergamon: 189–98.

Fries, Pascal. 2005. "A Mechanism for Cognitive Dynamics: Neuronal Communication Through Neuronal Coherence." *Trends in Cognitive Sciences* 9 (10). Elsevier: 474–80.

Fries, Pascal. 2015. "Rhythms for Cognition: Communication Through Coherence." *Neuron* 88 (1). Elsevier: 220–35.

Grech, Roberta, Tracey Cassar, Joseph Muscat, Kenneth P Camilleri, Simon G Fabri, Michalis Zervakis, Petros Xanthopoulos, Vangelis Sakkalis, and Bart Vanrumste. 2008. "Review on Solving the Inverse Problem in Eeg Source Analysis." *Journal of Neuroengineering and Rehabilitation* 5 (1). BioMed Central: 25.

Heuninckx, Sofie, Nicole Wenderoth, Filiep Debaere, Ronald Peeters, and Stephan P Swinnen. 2005. "Neural Basis of Aging: The Penetration of Cognition into Action Control." *Journal of Neuroscience* 25 (29). Soc Neuroscience: 6787–96.

Hjorth, Bo. 1975. "An on-Line Transformation of Eeg Scalp Potentials into Orthogonal Source Derivations." *Electroencephalography and Clinical Neurophysiology* 39 (5). Elsevier: 526–30.

Holme, Petter, and Jari Saramäki. 2012. "Temporal Networks." *Physics Reports* 519 (3): 97–125. https://doi.org/https://doi.org/10.1016/j.physrep.2012.03.001.

Kintali, Shiva. 2008. "Betweenness Centrality: Algorithms and Lower Bounds." *arXiv Preprint arXiv:0809.1906*.

Kronland-Martinet, Richard, Jean Morlet, and Alexander Grossmann. 1987. "Analysis of Sound Patterns Through Wavelet Transforms." *International Journal of Pattern Recognition and Artificial Intelligence* 1 (02). World Scientific: 273–302.

Lachaux, Jean-Philippe, Eugenio Rodriguez, Jacques Martinerie, and Francisco J Varela. 1999. "Measuring Phase Synchrony in Brain Signals." *Human Brain Mapping* 8 (4). Wiley Online Library: 194–208.

Liu, Liqing, Nils Rosjat, Svitlana Popovych, Bin A Wang, Azamat Yeldesbay, Tibor I Toth, Shivakumar Viswanathan, Christian B Grefkes, Gereon R Fink, and Silvia Daun. 2017. "Age-Related Changes in Oscillatory Power Affect Motor Action." *PloS One* 12 (11). Public Library of Science: e0187911.

Makeig, Scott, Anthony J Bell, Tzyy-Ping Jung, and Terrence J Sejnowski. 1996. "Independent Component Analysis of Electroencephalographic Data." In *Advances in Neural Information Processing Systems*, 145–51.

Meilă, Marina. 2007. "Comparing Clusterings—an Information Based Distance." *Journal of Multivariate Analysis* 98 (5). Elsevier: 873–95.

Mitrushina, Maura, and Paul Satz. 1991. "Analysis of Longitudinal Covariance Structures in Assessment of Stability of Cognitive Functions in Elderly." *Brain Dysfunction*. S Karger AG.

Nolde, Scott F, Marcia K Johnson, and Carol L Raye. 1998. "The Role of Prefrontal Cortex During Tests of Episodic Memory." *Trends in Cognitive Sciences* 2 (10). Elsevier: 399–406.

Oldfield, Richard C. 1971. "The Assessment and Analysis of Handedness: The Edinburgh Inventory." *Neuropsychologia* 9 (1). Elsevier: 97–113.

Palva, Satu, and J Matias Palva. 2012. "Discovering Oscillatory Interaction Networks with M/Eeg: Challenges and Breakthroughs." *Trends in Cognitive Sciences* 16 (4). Elsevier: 219–30.

Popovych, Svitlana, Nils Rosjat, Tibor Istvan Toth, Bin A Wang, L Liu, Rouhollah O Abdollahi, Shivakumar Viswanathan, Christian Grefkes, Gereon R Fink, and S Daun. 2016. "Movement-Related Phase Locking in the Delta–Theta Frequency Band." *NeuroImage* 139. Elsevier: 439–49.

Reichardt, Jörg, and Stefan Bornholdt. 2006. "Statistical Mechanics of Community Detection." *Physical Review E* 74 (1). APS: 016110.

Reuter-Lorenz, Patricia A, John Jonides, Edward E Smith, Alan Hartley, Andrea Miller, Christina Marshuetz, and Robert A Koeppe. 2000. "Age Differences in the Frontal Lateralization of Verbal and Spatial Working Memory Revealed by Pet." *Journal of Cognitive Neuroscience* 12 (1). MIT Press: 174–87.

Ronhovde, Peter, and Zohar Nussinov. 2009. "Multiresolution Community Detection for Megascale Networks by Information-Based Replica Correlations." *Physical Review E* 80 (1). APS: 016109.

Rosjat, Nils, Liqing Liu, Bin A Wang, Svitlana Popovych, Tibor Tóth, Shivakumar Viswanathan, Christian Grefkes, Gereon R Fink, and Silvia Daun. 2018. "Aging-Associated Changes of Movement-Related Functional Connectivity in the Human Brain." *Neuropsychologia* 117. Elsevier: 520–29.

Rubinov, Mikail, and Olaf Sporns. 2010. "Complex Network Measures of Brain Connectivity: Uses and Interpretations." *Neuroimage* 52 (3). Elsevier: 1059–69.

Sailer, Alexandra, Johannes Dichgans, and Christian Gerloff. 2000. "The Influence of Normal Aging on the Cortical Processing of a Simple Motor Task." *Neurology* 55 (7): 979–85.

Seidler, Rachael D., Jessica A. Bernard, Taritonye B. Burutolu, Brett W. Fling, Mark T. Gordon, Joseph T. Gwin, Youngbin Kwak, and David B. Lipps. 2010. "Motor control and aging: Links to age-related brain structural, functional, and biochemical effects." *Neuroscience & Biobehavioral Reviews* 34 (5). Pergamon: 721–33. https://doi.org/10.1016/J.NEUBIOREV.2009.10.005.

SINGER, W. 2004. "Synchrony, Oscillations, and Relational Codes." *The Visual Neurosciences*. The MIT Press, 1665–81. https://ci.nii.ac.jp/naid/10026657757/en/.

Singer, Wolf. 1999. "Neuronal Synchrony: A Versatile Code for the Definition of Relations?" *Neuron* 24 (1). Cell Press: 49–65. https://doi.org/10.1016/S0896-6273(00)80821-1.

Sizemore, Ann E, and Danielle S Bassett. 2018. "Dynamic Graph Metrics: Tutorial, Toolbox, and Tale." *NeuroImage* 180. Elsevier: 417–27.

Spreen, O., and E. Strauss. 1998. "A Compendium of Neuropsychological Tests: Administration, Norms and Commentary." In. Oxford University Press, New York.

Sun, Yudong, Bogdan Danila, K Josić, and Kevin E Bassler. 2009. "Improved Community Structure Detection Using a Modified Fine-Tuning Strategy." *EPL (Europhysics Letters)* 86 (2). IOP Publishing: 28004.

Uhlhaas, Peter J., Frédéric Roux, Eugenio Rodriguez, Anna Rotarska-Jagiela, and Wolf Singer. 2010. "Neural synchrony and the development of cortical networks." *Trends in Cognitive Sciences* 14 (2). Elsevier Current Trends: 72–80. https://doi.org/10.1016/J.TICS.2009.12.002.

Van Wijk, Bernadette C. M., Peter J. Beek, and Andreas Daffertshofer. 2012. "Neural synchrony within the motor system: what have we learned so far?" *Frontiers in Human Neuroscience* 6 (September). Frontiers: 252. https://doi.org/10.3389/fnhum.2012.00252.

Wang, Bin A., Shivakumar Viswanathan, R.O. Rouhollah O. Abdollahi, Nils Rosjat, Svitlana Popovych, Silvia Daun, Christian Grefkes, and Gereon R. Fink. 2017. "Frequency-specific modulation of connectivity in the ipsilateral sensorimotor cortex by different forms of movement initiation." *NeuroImage* 159 (October). Academic Press: 248–60. https://doi.org/10.1016/J.NEUROIMAGE.2017.07.054.

Ward, Nick S., Orlando B.C. Swayne, and Jennifer M. Newton. 2008. "Age-Dependent Changes in the Neural Correlates of Force Modulation: An fMRI Study." *Neurobiology of*

Aging 29 (9): 1434–46. https://doi.org/https://doi.org/10.1016/j.neurobiolaging.2007.04.017.

Wendel, Katrina, Outi Väisänen, Jaakko Malmivuo, Nevzat G. Gencer, Bart Vanrumste, Piotr Durka, Ratko Magjarević, et al. 2009. "EEG/MEG Source Imaging: Methods, Challenges, and Open Issues." *Computational Intelligence and Neuroscience* 2009: 1–12. https://doi.org/10.1155/2009/656092.

Wu, Tao, and Mark Hallett. 2005. "The influence of normal human ageing on automatic movements." *The Journal of Physiology* 562 (2): 605–15. https://doi.org/10.1113/jphysiol.2004.076042.